



Cite this: *Chem. Commun.*, 2024, 60, 4601

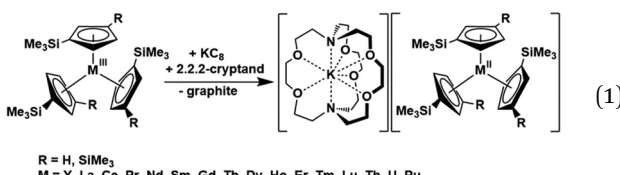
Received 5th March 2024,
Accepted 28th March 2024

DOI: 10.1039/d4cc01037j

rsc.li/chemcomm

To expand the range of donor atoms known to stabilize $4f^n5d^1$ $\text{Ln}(\text{II})$ ions beyond the C, N, and O first row main group donor atoms, the $\text{Ln}(\text{III})$ sulfur donor terphenylthiolate iodide complexes, $\text{Ln}^{\text{III}}(\text{SAr}^{\text{IPr}6})_2\text{I}$ ($\text{Ar}^{\text{IPr}6} = \text{C}_6\text{H}_3\text{-2,6-(C}_6\text{H}_2\text{-2,4,6-}^{\text{I}}\text{Pr}_3)_2$, $\text{Ln} = \text{La, Nd}$) were reduced to form $\text{Ln}^{\text{II}}(\text{SAr}^{\text{IPr}6})_2$ complexes. These $\text{Ln}(\text{II})$ species were structurally characterized, analyzed by density functional theory (DFT) calculations, and compared to $\text{Tm}(\text{SAr}^{\text{IPr}6})_2$, which was synthesized from $\text{TmI}_2(\text{DME})_3$.

Recent developments in the redox chemistry of the rare-earth metals have shown that molecular complexes of the $4f^n$ $\text{Ln}(\text{III})$ ions can be reduced not only to $4f^{n+1}$ $\text{Ln}(\text{II})$ complexes for Eu, Yb, Sm, Tm, Dy, and Nd, but also to $4f^n5d^1$ $\text{Ln}(\text{II})$ ions of all the other lanthanides (except radioactive Pm). Complexes of $4d^1$ $\text{Y}(\text{II})$ can also be obtained.⁴ Many variations in ligands have been found to stabilize the new $4f^n5d^1$ $\text{Ln}(\text{II})$ complexes since Lappert, *et al.* reported the first examples with La and Ce in 2008¹ and examples for the rest of the lanthanides were described in 2013,² eqn (1). $\text{Nd}(\text{II})$ and $\text{Dy}(\text{II})$ are configurational crossover ions which can display $4f^{n+1}$ or $4f^n5d^1$ electron configurations depending on the specific ligand.⁵



Although this new $\text{Ln}(\text{II})$ chemistry has been extended to a variety of other ligands,^{6–12} they all involve C, N and O

Department of Chemistry, University of California, Irvine, California 92697, USA.
E-mail: wevans@uci.edu

† Electronic supplementary information (ESI) available. CCDC 2261276, 2296619, 2336642, 2296620, 2322910, 2326839 and 2328071. For ESI and crystallographic data in CIF or other electronic format see DOI: <https://doi.org/10.1039/d4cc01037j>

‡ These authors contributed equally to this work.

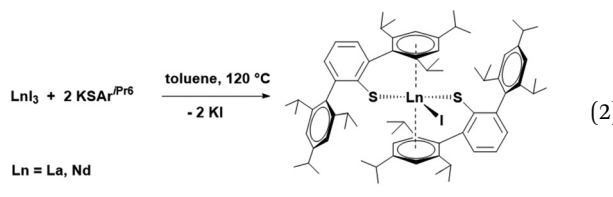
donor atoms from the first row of the main group. It was therefore of interest to determine if the new $\text{Ln}(\text{II})$ ions could be stabilized with second row donor atoms.¹³ Our focus turned to arylthiolates since we had found previously that the aryloxide, OAr^* [$\text{Ar}^* = \text{C}_6\text{H}_2\text{-2,6-(1-adamantyl)-4-}^{\text{t}}\text{Bu}$] provides some of the most thermally stable complexes of the $4f^n5d^1$ $\text{Ln}(\text{II})$ ions.¹⁰

The terphenylthiolate ligand, $\text{SAr}^{\text{IPr}6}$ [$\text{Ar}^{\text{IPr}6} = \text{C}_6\text{H}_3\text{-2,6-(C}_6\text{H}_2\text{-2,4,6-}^{\text{I}}\text{Pr}_3)_2$], was attractive because Power, *et al.* had previously shown the efficacy of this ligand framework to stabilize two-coordinate $\text{M}(\text{II})$ thiolate complexes of Si, Ge, Sn, and Pb,¹⁴ as well as Cr, Mn, Fe, Co, Ni, and Zn^{15} and Mg.¹⁶ Furthermore, with the $\text{NHAr}^{\text{IPr}6}$ analog, formally two-coordinate $\text{M}(\text{II})$ complexes were isolated for V,¹⁷ Cr,¹⁸ Mn,¹⁹ Fe,²⁰ Co,²¹ and Ni.²¹

The hexa-iso-propyl terphenylthiolate ligand also had been used in the rare-earth area. Niemeyer, *et al.* isolated $\text{Ln}(\text{SAr}^{\text{IPr}6})_2$ complexes for the traditional $4f^{n+1}$ $\text{Ln}(\text{II})$ ions, namely, Sm,²² Eu,²³ and Yb,²⁴ as well as the THF and DME solvates, $(\text{Ar}^{\text{IPr}6}\text{S})_2\text{Yb}(\text{THF})_4$ ²⁵ and $(\text{Ar}^{\text{IPr}6}\text{S})_2\text{Yb}(\text{DME})_2$.²⁴ The $\text{OAr}^{\text{IPr}6}$ analog was used to synthesize $\text{Sm}(\text{OAr}^{\text{IPr}6})_2$,²⁶ while the $\text{NHAr}^{\text{IPr}6}$ ligand was used to generate $\text{U}(\text{NHAr}^{\text{IPr}6})_2$ ²⁷ and $\text{Y}(\text{NHAr}^{\text{IPr}6})_2$.⁸ We report here the expansion of the initially reported $\text{Ln}(\text{SAr}^{\text{IPr}6})_2$ series to La, Nd, and Tm. These metals were examined since La(II) has a distinctive EPR spectrum, Nd(II) is a configurational crossover ion,⁵ and Tm was an unreported example of the $4f^{n+1}$ series.

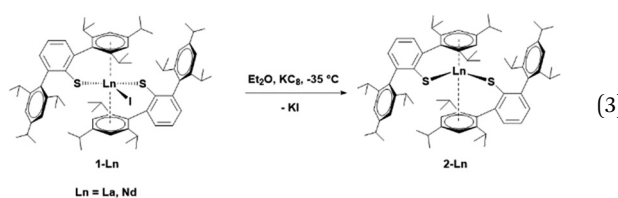
The $\text{Ln}(\text{SAr}^{\text{IPr}6})_2\text{I}$ complexes of $\text{Ln} = \text{La}$ and Nd were prepared by reaction of $\text{KSAr}^{\text{IPr}6}$ ^{28,29} with LnI_3 , eqn (2). The **1-Ln** complexes (see ESI† for structures) are structurally similar to and crystallize in the same space group and with nearly identical unit cell constants as the previously reported $\text{Eu}(\text{SAr}^{\text{IPr}6})_2\text{Cl}$ ³⁰ complex, the $\text{Ln}(\text{SAr}^{\text{IPr}6})_2$ complexes of $\text{Ln} = \text{Sm}$,²² and Eu,³⁰ and the $\text{Ln}(\text{SeAr}^{\text{IPr}6})_2\text{Cl}$ complexes of $\text{Ln} = \text{Nd}$ ³⁰ and Pr.³⁰ Evidently, the steric bulk of two $\text{SAr}^{\text{IPr}6}$ ligands is sufficient to generate the overall

molecular structure independent of the rare-earth metal and the presence or absence of a halide ligand.



The flanking arene rings of each $\text{SAr}^{\text{iPr}6}$ ligand in the **1-Ln** compounds are oriented toward the metal to form a sandwich-like structure for the **1-Ln** compounds. The $\text{La}-\text{C}_{\text{nt}}$ distances of 2.809(2) and 2.817(2) Å and the $\text{Nd}-\text{C}_{\text{nt}}$ distances of 2.799(1) and 2.793(1) Å ($\text{C}_{\text{nt}} = \text{flanking arene ring centroid}$) are more similar than the difference between the radii of the metal ions ($\text{La} = 1.216$ Å, $\text{Nd} = 1.163$ Å).³¹ The $\text{C}_{\text{nt1}}-\text{Ln}-\text{C}_{\text{nt2}}$ angles are 173.22(5)° for **1-La** and 175.38(1)° for **1-Nd**.

Treatment of Et_2O solutions of **1-Ln** chilled to -35 °C with slurries of KC_8 in Et_2O at -35 °C generated intensely dark brown solutions for both La and Nd. Recrystallization of the products from hexane at -35 °C produced brown blocks of $\text{Ln}(\text{SAr}^{\text{iPr}6})_2$, **2-Ln**, in 80% (La) and 70% (Nd) yield, eqn (3), which were identified by X-ray crystallography. The stability of the **2-Ln** complexes in hexane solution was monitored by UV-vis spectroscopy. The absorption of **2-La** at 409 nm decreases by only 25% over 24 h. For **2-Nd** at 274 nm, the decrease was 5% in 36 h.



The **2-Ln** complexes crystallize in the same space group as the **1-Ln** complexes and for both La and Nd, there is residual unreacted **1-Ln** co-crystallized with **2-Ln**. The amount of **1-Ln** contained in the samples of **2-Ln** varied from 13% to 84%. Longer reaction times, using THF as an alternative solvent, and performing reactions in the presence of 2,2,2-cryptand (crypt) and 18-crown-6 (18-c-6) did not solve the iodide contamination problem.

However, iodide-free **2-Nd** could be prepared in 70% yield through an alternate route by the reaction of NdI_2 ^{32,33} with $\text{KSAr}^{\text{iPr}6}$ in Et_2O over two days at room temperature. This synthesis was modeled on a reaction of $\text{TmI}_2(\text{DME})_3$ and of $\text{KSAr}^{\text{iPr}6}$ in Et_2O which provided the previously unreported **2-Tm**, eqn (4). The structure of **2-Tm** is similar to the previously reported **2-Sm**, **2-Eu**, and **2-Yb** and the $\text{Ln}-\text{S}$ bond distances scale like the ionic radii (Table S10, ESI†). In all of these complexes, both flanking rings of the $\text{SAr}^{\text{iPr}6}$ ligand sandwich the metal. In **2-Tm**, the $\text{Ln}-\text{C}_{\text{nt}}$ distances are 2.642(1) and 2.663(1) Å and the $\text{C}_{\text{nt}}-\text{Ln}-\text{C}_{\text{nt}}$ angle is 164.09(3)°.

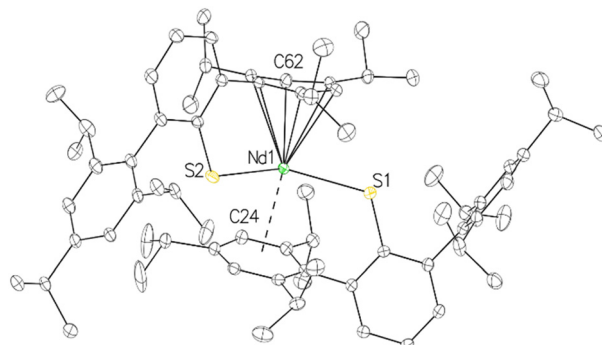
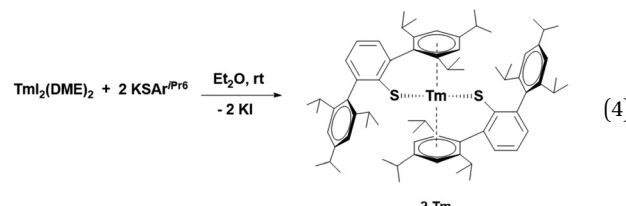


Fig. 1 The molecular structure of $\text{Nd}(\text{SAr}^{\text{iPr}6})_2$, **2-Nd**, with thermal ellipsoids drawn at 30% probability. For clarity, hydrogen atoms and the minor components of modeled disorder (isopropyl substituents, 20% site disorder of Nd atom) are not shown.



The molecular structure of **2-Nd** is shown in Fig. 1 and the structurally similar **2-La** (including the *ca.* 13% crystallographic iodide impurity) is shown Fig. S39 (ESI†). **2-La** and **2-Nd** differ from **1-Ln** and the other **2-Ln** structures ($\text{Ln} = \text{Sm, Eu, Tm, and Yb}$) in that one flanking ring of a terphenyl ligand is substantially closer to the Ln ion than the other. **2-La** has $\text{La}-\text{C}_{\text{nt}}$ distances of 2.524(4) and 2.808(5) Å; for **2-Nd**, they are 2.395(1) and 2.804(1) Å. In both **2-La** and **2-Nd**, the ring that is closer to the Ln ion has a boat-like distortion from planarity. The $\text{C}-\text{C}$ distances in the proximal ring of **2-Ln** do not differ as widely as those of fully reduced arene rings as detailed in Fig. S54 (ESI†), although a range of distances has been observed in reduced arene complexes.^{34–39}

The EPR spectra of THF solutions of **2-La** (Fig. 2) and $\text{La}(\text{SAr}^{\text{iPr}6})_2\text{I}/\text{KC}_8/\text{chelate}$ reaction products (Table S1 and Fig. S43, ESI†) at room temperature have eight-line patterns characteristic of $\text{La}(\text{II})$. The spectrum of **2-La** was fitted using EasySpin⁴⁰ which indicated $g = 1.99$ and $A = 67.3$ MHz (22.9 G). The g value is similar to all previously reported $\text{La}(\text{II})$ complexes, but the A value is smaller: (g , A MHz) $\{\text{La}[\text{C}_5\text{H}_3(\text{SiMe}_3)_2]_3\}^{1-}$ (1.99, 372);¹ $[\text{La}(\text{C}_5\text{H}_4\text{SiMe}_3)_3]^{1-}$ (1.994, 430.4);⁴¹ $[\text{La}(\text{C}_5\text{H}_4\text{Me})_3]^{1-}$ (1.971, 537.9);⁴² $[\text{La}(\text{C}_5\text{H}_4\text{^tBu})_3]^{1-}$ (1.959, 559 MHz);⁴³ $\{\text{La}[\text{C}_5\text{H}_4(\text{^tBu})_2]_3\}^{1-}$ (1.977, 642.8);⁴⁴ $[\text{La}(\text{C}_5\text{HMe}_4)_3]^{1-}$ (1.97, 802);⁴⁵ $[\text{La}[\text{OC}_6\text{H}_2-2,6-(1\text{-Ad})_2-4-\text{tBu}]_3]^{1-}$ (2.00, 1840).⁴⁶ We note that in $[\text{K}(\text{crypt})][\text{U}(\text{TDA})_2]$ ($\text{TDA} = \text{N}-(2,6\text{-di-isopropylphenyl})\text{pivalamido}$), which contains a monoreduced arene in one of the TDA ligands, a nearly axial single-line EPR signal is observed with $g = [2.042, 2.021, 2.013]$ which is assigned to the arene radical anion.³⁹ The EPR spectrum of a solid sample of **2-La** (Fig. S44, ESI†) displayed a single broad

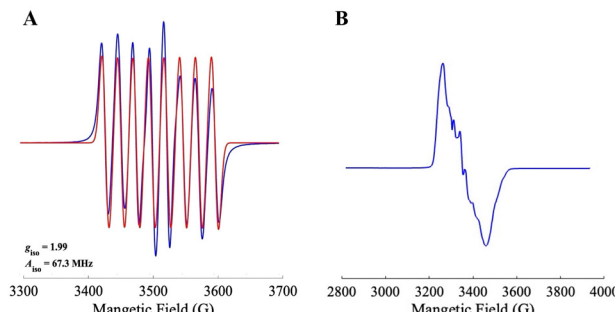


Fig. 2 EPR spectra at 298 K (A) and 77 K (B) of **2-La**. The blue traces are experimental spectra and the red trace was fitted from the experimental data using EasySpin. The g and hyperfine coupling constants determined at 298 K are $g_{\text{iso}} = 1.99$ and $A_{\text{iso}} = 67.3$ MHz (24.2 Gauss). EPR data for the $\text{La}(\text{SAr}^{\text{IPr}^6})_2\text{I}/\text{KC}_8/18\text{-c-6}$ and $\text{La}(\text{SAr}^{\text{IPr}^6})_2\text{I}/\text{KC}_8/\text{crypt}$ reaction products can be found in Table S1 and Fig. S43 (ESI†).

signal with $g = 1.98$ and no resolved hyperfine coupling similar to that of the $\text{La}(\text{n})$ complex $[\text{K}(\text{crown})][\text{LaCp}_3'']$ ($\text{Cp}'' = \eta^5\text{-1,3-(SiMe}_3)_2\text{-C}_5\text{H}_3$).¹

Density functional theory calculations were carried out to evaluate the electronic structure of the **2-Ln** complexes at the TPSSh-D3(BJ)/def2-TZVP level of theory (see ESI† for computational details). Calculations starting with the X-ray crystal structure of **2-La** gave a symmetric structure with 2.572 and 2.597 Å La-Cnt distances (Table S11, ESI†). When the higher quality X-ray crystal structure of **2-Nd** was used and the metal changed to La, the calculations converged to a local minimum with an asymmetric structure with 2.487 and 2.742 Å La-Cnt distances. The symmetric structure is only 0.37 kcal mol⁻¹ more stable than the asymmetric structure. The 80.1 MHz hyperfine coupling constants calculated for the symmetric structure of **2-La** (Table S14, ESI†) are closer to the 67.3 MHz experimental value than the 182.1 MHz values calculated for the asymmetric structure. Hence, the symmetric structure fits the experimental EPR data best and the asymmetric structure matches the crystal data. The SOMO for the symmetric structure of **2-La** (Fig. S55, ESI†) has a Mulliken population analysis with 34.4% 5d, 36.0% arene p orbitals, and only 4.3% s character. This is consistent with the smaller hyperfine coupling constant observed for **2-La** compared to other $\text{La}(\text{n})$ complexes. For **2-Nd**, Mulliken population analysis shows distinct f character (90%+) for α HOSO-3, α HOSO-2, and α HOSO-1, but it is only 61.5% for α HOSO with most of the remaining character (23.3%) being described by the six carbon p-orbitals involved in the δ -type interaction (Fig. S58, ESI†). Hence, this is not a $4f^35d^1$ Nd(n) ion and a $4f^4$ designation with significant electron transfer to the ring is a more appropriate description. Nd(n) is a known configurational crossover ion that can have these two different electron configurations depending on the ligand set.^{5,41} Additional calculations on a truncated model complex $\text{Nd}(\text{SH})_2\text{-(C}_6\text{H}_6)_2$ and its fragments $\text{Nd}(\text{SH})_2$ and $(\text{C}_6\text{H}_6)_2$ suggest that the α HOSO is obtained by dative bonding of two π^* orbitals of the arene fragments and the f_{xyz} orbital of Nd (Fig. S60, ESI†).

The reductive chemistry of **2-Nd** was examined by treating it with azobenzene. The reaction forms $\text{Nd}^{\text{III}}(\text{SAr}^{\text{IPr}^6})_2(\text{PhNNPh})$,

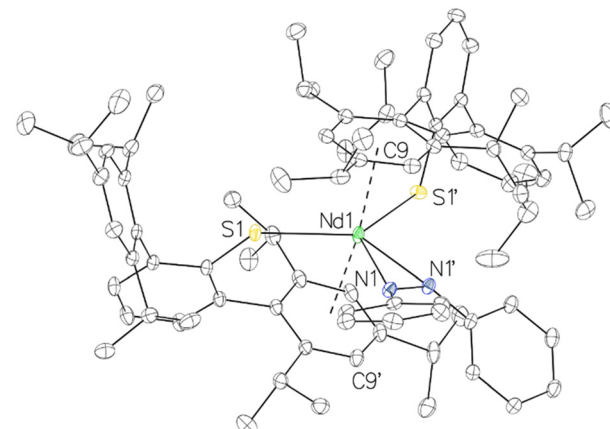
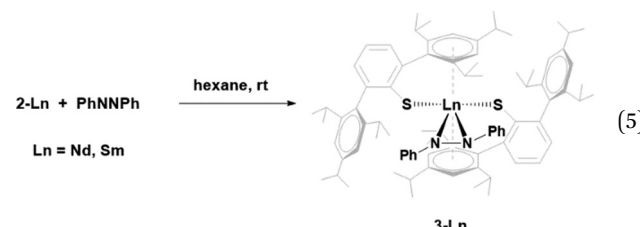


Fig. 3 The molecular structure of $\text{Nd}(\text{SAr}^{\text{IPr}^6})_2(\text{PhNNPh})$, **3-Nd**, with thermal ellipsoids drawn at 30% probability. For clarity, hydrogen atoms and minor components of modeled disorder in two isopropyl substituents are not shown.

3-Nd, eqn (5), Fig. 3, which has structural and spectroscopic features characteristic of $\text{Ln}(\text{m})$ complexes containing $(\text{PhNNPh})^{1-}$ anions (see ESI†).⁴⁷⁻⁴⁹ The reaction of **2-Sm** with azobenzene gives the analogous compound, **3-Sm** (see ESI†). The structure of **3-Nd** demonstrates the steric flexibility of the $\text{SAr}^{\text{IPr}^6}$ ligand which can obviously change the orientation of the flanking arene rings to accommodate a ligand as large as $(\text{PhNNPh})^{1-}$.



In summary, sulfur donor atom ligands can be used to isolate $\text{La}(\text{n})$ and $\text{Nd}(\text{n})$ ions, but with the $\text{SAr}^{\text{IPr}^6}$ ligand this involves partial reduction of a flanking arene ring. This apparently stabilizes the complexes compared to other $\text{La}(\text{n})$ and $\text{Nd}(\text{n})$ complexes and may make them better reagents for $\text{Ln}(\text{n})$ reductive chemistry. The reaction of **2-Nd** with azobenzene shows that it is a competent one electron reductant equivalent to the traditional rare-earth reductant $\text{Sm}(\text{n})$.⁵⁰ In the case of **2-Nd**, the DFT analysis suggests a $4f^4$ electron configuration rather than $4f^35d^1$. This is consistent with complexes such as $[\text{K}(\text{crypt})_2[(\text{KX}_3\text{Ce})(\text{C}_6\text{H}_5\text{Me})_2]\text{Ce}]$ [X = $\text{OSi}(\text{O}^{\text{t}}\text{Bu})_3$]⁶, $[\text{K}(\text{crypt})][(\text{Ad},\text{MeArO})_3\text{U}]$,⁵¹ $(\text{NHAr}^{\text{IPr}^6})_2\text{U}$,²⁷ and $[\text{K}(\text{crypt})][\text{U}(\text{TDA})_2]$ ³⁹ which contain arene rings near a metal ion in the +2 oxidation state and are assigned f^{n+1} electron configurations instead of f^nd^1 configurations.

The authors thank the U. S. National Science Foundation for support of this research under CHE-2154255 (W. J. E.) and CHE-2102568 (F. F.). R. G. acknowledges support *via* a Walter-Benjamin postdoctoral fellowship funded by the Deutsche

Forschungsgemeinschaft (DFG, German Research Foundation) - 501114520. We also thank Professor A. S. Borovik and Phan Phu for assistance with EPR spectroscopy and Joseph Q. Nguyen and Lauren Andersen-Sanchez for assistance with elemental analyses.

Conflicts of interest

The authors declare no competing financial interest. Principal Investigator Filipp Furche has an equity interest in TURBOMOLE GmbH. The terms of this arrangement have been reviewed and approved by the University of California, Irvine, in accordance with its conflict of interest policies.

References

- P. B. Hitchcock, M. F. Lappert, L. Maron and A. V. Protchenko, *Angew. Chem., Int. Ed.*, 2008, **47**, 1488–1491.
- M. R. MacDonald, J. E. Bates, J. W. Ziller, F. Furche and W. J. Evans, *J. Am. Chem. Soc.*, 2013, **135**, 9857–9868.
- W. J. Evans, *Organometallics*, 2016, **35**, 3088–3100.
- M. R. MacDonald, J. W. Ziller and W. J. Evans, *J. Am. Chem. Soc.*, 2011, **133**, 15914–15917.
- M. E. Fieser, C. T. Palumbo, H. S. La Pierre, D. P. Halter, V. K. Voora, J. W. Ziller, F. Furche, K. Meyer and W. J. Evans, *Chem. Sci.*, 2017, **8**, 7424–7433.
- R. P. Kelly, L. Maron, R. Scopelliti and M. Mazzanti, *Angew. Chem., Int. Ed.*, 2017, **56**, 15663–15666.
- K. R. McClain, C. A. Gould, D. A. Marchiori, H. Kwon, T. T. Nguyen, K. E. Rosenkoetter, D. Kuzmina, F. Tuna, R. D. Britt, J. R. Long and B. G. Harvey, *J. Am. Chem. Soc.*, 2022, **144**, 22193–22201.
- R. Jena, F. Benner, F. Delano, D. Holmes, J. McCracken, S. Demir and A. L. Odom, *Chem. Sci.*, 2023, **14**, 4257–4264.
- Y. Wang, J. Liang, C. Deng, R. Sun, P.-X. Fu, B.-W. Wang, S. Gao and W. Huang, *J. Am. Chem. Soc.*, 2023, **145**, 22466–22474.
- L. M. Anderson-Sanchez, J. M. Yu, J. W. Ziller, F. Furche and W. J. Evans, *Inorg. Chem.*, 2023, **62**, 706–714.
- A. J. Ryan, J. W. Ziller and W. J. Evans, *Chem. Sci.*, 2020, **11**, 2006–2014.
- C. T. Palumbo, D. P. Halter, V. K. Voora, G. P. Chen, A. K. Chan, M. E. Fieser, J. W. Ziller, W. Hieringer, F. Furche, K. Meyer and W. J. Evans, *Inorg. Chem.*, 2018, **57**, 2823–2833.
- D. Pividori, M. E. Miehlich, B. Kestel, F. W. Heinemann, A. Scheurer, M. Patzschke and K. Meyer, *Inorg. Chem.*, 2021, **60**, 16455–16465.
- B. D. Rekken, T. M. Brown, J. C. Fettinger, F. Lips, H. M. Tuononen, R. H. Herber and P. P. Power, *J. Am. Chem. Soc.*, 2013, **135**, 10134–10148.
- T. Nguyen, A. Panda, M. M. Olmstead, A. F. Richards, M. Stender, M. Brynda and P. P. Power, *J. Am. Chem. Soc.*, 2005, **127**, 8545–8552.
- M. Niemeyer and P. P. Power, *Inorg. Chim. Acta*, 1997, **263**, 201–207.
- J. N. Boynton, J.-D. Guo, J. C. Fettinger, C. E. Melton, S. Nagase and P. P. Power, *J. Am. Chem. Soc.*, 2013, **135**, 10720–10728.
- J. N. Boynton, W. A. Merrill, W. M. Reiff, J. C. Fettinger and P. P. Power, *Inorg. Chem.*, 2012, **51**, 3212–3219.
- C. Ni, B. Rekken, J. C. Fettinger, G. J. Long and P. P. Power, *Dalton Trans.*, 2009, 8349–8355.
- W. A. Merrill, T. A. Stich, M. Brynda, G. J. Yeagle, J. C. Fettinger, R. De Hont, W. M. Reiff, C. E. Schulz, R. D. Britt and P. P. Power, *J. Am. Chem. Soc.*, 2009, **131**, 12693–12702.
- A. M. Bryan, W. A. Merrill, W. M. Reiff, J. C. Fettinger and P. P. Power, *Inorg. Chem.*, 2012, **51**, 3366–3373.
- A. Cofone and M. Niemeyer, *Z. Anorg. Allg. Chem.*, 2006, **632**, 1930–1932.
- J. Angelkort, S. van Smaalen, S. O. Hauber and M. Niemeyer, *Z. Anorg. Allg. Chem.*, 2007, **633**, 1031–1035.
- M. Niemeyer, *Eur. J. Inorg. Chem.*, 2001, 1969–1981.
- M. Niemeyer, *Acta Crystallogr., Sect. E: Crystallogr. Commun.*, 2001, **57**, m396–m398.
- P. Zhao, Q. Zhu, J. C. Fettinger and P. Power, *Inorg. Chem.*, 2018, **57**, 14044–14046.
- B. S. Billow, B. N. Livesay, C. C. Mokhtarzadeh, J. McCracken, M. P. Shores, J. M. Boncella and A. L. Odom, *J. Am. Chem. Soc.*, 2018, **140**, 17369–17373.
- M. Niemeyer and P. P. Power, *Inorg. Chem.*, 1996, **35**, 7264–7272.
- J. K. Pratt, P. P. Power, N. D. Mendelson and J. S. Figueroa, *Inorg. Synth.*, 2018, **37**, 116–120.
- S.-O. Hauber and M. Niemeyer, *Chem. Commun.*, 2007, 275–277.
- R. D. Shannon, *Acta Crystallogr., Sect. A: Cryst. Phys., Diffr., Theor. Gen. Crystallogr.*, 1976, **32**, 751–767.
- M. N. Bochkarev and A. A. Fagin, *Chem. – Eur. J.*, 1999, **5**, 2990–2992.
- W. J. Evans, N. T. Allen, P. S. Workman and J. C. Meyer, *Inorg. Chem.*, 2003, **42**, 3097–3099.
- P. B. Hitchcock, M. F. Lappert and A. V. Protchenko, *J. Am. Chem. Soc.*, 2001, **123**, 189–190.
- J. N. Boynton, J.-D. Guo, F. Grandjean, J. C. Fettinger, S. Nagase, G. J. Long and P. P. Power, *Inorg. Chem.*, 2013, **52**, 14216–14223.
- S. M. Hubig, S. V. Lindeman and J. K. Kochi, *Coord. Chem. Rev.*, 2000, **200**–**202**, 831–873.
- S. V. Rosokha and J. K. Kochi, *Mod. Arene Chem.*, 2002, 435–478.
- I. L. Fedushkin, M. N. Bochkarev, H. Schumann and L. Esser, *J. Organomet. Chem.*, 1995, **489**, 145–151.
- M. D. Straub, E. T. Ouellette, M. A. Boreen, R. D. Britt, K. Chakarawet, I. Douair, C. A. Gould, L. Maron, I. Del Rosal, D. Villarreal, S. G. Minasian and J. Arnold, *J. Am. Chem. Soc.*, 2021, **143**, 19748–19760.
- S. Stoll and A. Schweiger, *J. Magn. Reson.*, 2006, **178**, 42–55.
- M. E. Fieser, M. R. MacDonald, B. T. Krull, J. E. Bates, J. W. Ziller, F. Furche and W. J. Evans, *J. Am. Chem. Soc.*, 2015, **137**, 369–382.
- D. H. Woen, D. N. Huh, J. W. Ziller and W. J. Evans, *Organometallics*, 2018, **37**, 3055–3063.
- M. A. Angadol, D. H. Woen, C. J. Windorff, J. W. Ziller and W. J. Evans, *Organometallics*, 2019, **38**, 1151–1158.
- J. Liu, L. E. Nodaraki, D. O. Martins, M. J. Giansiracusa, P. J. Cobb, J. Emerson-King, F. Ortú, G. F. Whitehead, G. K. Gransbury, E. J. McInnes, F. Tuna and D. P. Mills, *Eur. J. Inorg. Chem.*, 2023, e202300552.
- T. F. Jenkins, D. H. Woen, L. N. Mohanam, J. W. Ziller, F. Furche and W. J. Evans, *Organometallics*, 2018, **37**, 3863–3873.
- K. Kundu, J. R. K. White, S. A. Moehring, J. M. Yu, J. W. Ziller, F. Furche, W. J. Evans and S. Hill, *Nat. Chem.*, 2022, **14**, 392–397.
- W. J. Evans and D. K. Drummond, *J. Am. Chem. Soc.*, 1986, **108**, 7440–7441.
- W. J. Evans, D. K. Drummond, S. G. Bott and J. L. Atwood, *Organometallics*, 1986, **5**, 2389–2391.
- W. J. Evans, D. K. Drummond, L. R. Chamberlain, R. J. Doedens, S. G. Bott, H. Zhang and J. L. Atwood, *J. Am. Chem. Soc.*, 1988, **110**, 4983–4994.
- W. J. Evans and D. K. Drummond, *J. Am. Chem. Soc.*, 1989, **111**, 3329–3335.
- H. S. La Pierre, A. Scheurer, F. W. Heinemann, W. Hieringer and K. Meyer, *Angew. Chem., Int. Ed.*, 2014, **53**, 7158–7162.